Embryonic and Early Larval Development of the Pacific Razor Clam (*Siliqua patula*)

Marina W. Alcantar[1,*], Jeff Hetrick[2], Jacqueline Ramsay[2], and Amanda L. Kelley[1]

[1] College of Fisheries and Ocean Sciences, University of Alaska Fairbanks, Fairbanks, Alaska 99775
[2] Alutiiq Pride Marine Institute, Seward, Alaska 99664

Abstract

The Pacific razor clam, Siliqua patula *(Sugpiaq: Cingtaataq, Dixon, 1789), is vital to commercial, recreational, and subsistence fisheries across the Pacific Northwest Coast of North America. Despite the species' status as one of the most popular shellfish species harvested in the Pacific Northwest, British Columbia, and Alaska, its larval development has never been fully characterized. Generating a developmental times series, and describing development fully, is crucial for guiding targeted management, developing a mariculture strategy for the species, and providing a more pointed avenue for studies examining the response of* S. patula *to ocean change. This study presents the first photographic documentation of larval development in* S. patula*, including the timing of key transitions during embryogenesis and early larval development. Scanning electron microscopy revealed that the larval shell forms* via *a concretion, a process typically documented in early gastropod development. This novel characterization is pertinent, as it conveys the need for the inclusion of alternative bivalve development processes, such as a concretion, in bivalve research. This study also compared development in* S. patula *to a global assortment of bivalve species, including two other members of the Pharidae family, determining that the timing to D-veliger and trochophore stages was similar to the majority of bivalves surveyed. While bivalve response to climate change is a topic of great interest, not all species of concern have undergone comprehensive developmental assessments, a requisite benchmark for designing climate change studies that examine early life history sensitivity to such changes. This research supports the use of comprehensive developmental studies as prerequisites for designing climate change experimentation, establishes the necessity of high-magnification and high-resolution scanning electron microscopy within developmental assessments, and provides information about the development of a cornerstone bivalve species.*

Introduction

The Pacific razor clam, *Siliqua patula* (Sugpiaq: Cingtaataq, Dixon, 1789), a member of the Pharidae family, is a popular shellfish species for coastal peoples, supporting commercial, recreational, and subsistence harvests across the Pacific Northwest (PNW) coast of North America. Millions of *S. patula* are harvested commercially in Alaska, Washington, and Oregon (Forster, 2019; Alaska Department of Fish and Game, 2020; Hunter, 2024), with the combined fisheries worth over $70 million (Ayres, 2022). In addition to its commercial value, *S. patula* is one of the most popular recreationally harvested shellfish in Alaska and the PNW (Alaska Department of Fish and Game, 2020; Swanson, 2024). Notably, the eastern Cook Inlet, Alaska, stock of *S. patula* has exhibited recent population declines, the cause of which is still unknown (Olsen, 2015). Given their wide distribution, *S. patula* experiences a wide variety of environmental conditions. In Cook Inlet, they experience a much colder and fresher environment, with temperatures ranging from −1 to 18 °C and salinities of 15–32 (Holderied and Baird, 2020; Miller and Kelley, 2021), compared to *S. patula* living along the Oregon coastline, which experience temperatures from 6 to 22 °C and salinities of 32–34 (Huang *et al.*, 2021; NOAA, 2023). In addition to being

Received 19 October 2023; Accepted 2 April 2024; Published online 30 May 2024.
* Corresponding author; email: mwalcantar@alaska.edu.
Abbreviations: DPF, days postfertilization; HPF, hours postfertilization; PDI, prodissoconch I; PNW, Pacific Northwest.

The Biological Bulletin, October 2023, volume 245, number 2: 57–67. https://doi.org/10.1086/730784

a resource for humans, *S. patula* is also a food source for multiple species of fish and crabs and a variety of sea birds (Alaska Department of Fish and Game, 2020).

Despite the value of *S. patula* to both humans and the ecosystem in which this species resides, details of the early development of the species are almost entirely unknown. For *S. patula*, a single development study was conducted to establish best practices for mariculture production. However, it did not fully document developmental timing, growth, or shell formation during the early larval stages (Breese and Robinson, 1981). To date, only three peer-reviewed studies have described the embryogenesis and larval development of other members of the Pharidae family (Breese and Robinson, 1981; Da Costa *et al.*, 2008, 2010). The Pharidae family is composed of six genera, all colloquially classified as razor clams, occupying intertidal zones with sandy substrate. All Pharidae taxa share similar physical characteristics (*e.g.*, elongated shells, pronounced digging foot, and a weak adductor muscle) and are widely dispersed, ranging from tropical to subarctic regions (Phoa Lee Na, 2008; Da Costa *et al.*, 2010). Their wide distribution has contributed to their use as a global, commercial, recreational, and subsistence resource (Da Costa *et al.*, 2008, 2010; Alaska Department of Fish and Game, 2020). Characterizing the developmental pathway and timing of *S. patula* is essential to inform future research and to potentially identify the vulnerability of this species to climate change and other environmental stressors.

The larval development of *S. patula* has been assumed to follow patterns commonly observed in other broadcast-spawning bivalves (McMillin, 1924). The bivalve embryonic phase can last anywhere from a few hours to a few days (Dorit *et al.*, 1991) and is temperature dependent (McEdward, 1985; Garcia de Severeyn *et al.*, 2000). Bivalves exhibit spiral holoblastic cleavage during early cell division (Gilbert, 2000), eventually reaching a 16-cell morula phase. The morula develops into the coeloblastula, where gastrulation begins to form the large blastocoel (Ponder *et al.*, 2019). After embryogenesis, individuals hatch into ciliated, free-swimming trochophore larvae, initiating the planktonic dispersal phase. The trochophore stage lasts 2 to 3 days, during which shell development typically begins (Hedgecock, 1995; Gros *et al.*, 1997; Ponder *et al.*, 2019). Completion of the trochophore stage is signaled by the formation of two complete valves, resulting in a straight-hinged, D-shaped veliger (Ponder *et al.*, 2019). The veliger stage ends when individuals settle out of the water column and undergo transformation into sessile juveniles. The total length of the veliger phase is species specific and is dependent on the shell formation approach, temperature, and veliger feeding strategy (Ponder *et al.*, 2019).

The objective of this study was to document developmental stages and timing in *S. patula*, with the broader goal of supporting future experimental work testing the effects of environmental stressors on *S. patula* larvae. Additionally, the application of high-magnification and high-resolution imaging was incorporated to document *S. patula* shell development, as light microscopy is potentially insufficient for the comprehensive characterization of mollusc shell development (Eyster and Morse, 1984). This research strengthens our understanding of early life history in the Pharidae family, and by characterizing the development of *S. patula*, this study has established a baseline for all future research. Furthermore, the results from this study will help inform decisions regarding the management and mariculture practices of this species.

Materials and Methods

Animal collection and husbandry

Adult *Siliqua patula* (Dixon, 1789) were harvested at Polly Creek Beach, located on the west side of Cook Inlet (60°16′54.9″ N, 152°27′40.5″ W), Alaska, on June 28, 2018. About 100 adult individuals, ranging in size from 10 to 13 cm, were gathered by commercial diggers from Pacific Seafood, Nikiski, Alaska, and transported in a cooler to the Alutiiq Pride Marine Institute, in Seward, Alaska, the same day of harvest. Individuals were inspected, and those with shell damage were excluded from the study group. The remaining individuals were rubber banded (according to hatchery protocol to mimic the influence of substrate pressure experienced *in situ*) and held in a 380-L flow-through tank. Hatchery seawater was sand filtered, UV treated, and mechanically filtered to 5 μm before entering 30,000-L temperature-controlled holding tanks.

For this study, two different larval cohorts of wild-caught *S. patula* were produced and maintained in the laboratory. Using the first cohort, timing and growth rates for different developmental stages were established. The second cohort was used for scanning electron microscopy and growth of the larval shell. Both cohorts were spawned using the same protocol and were cultured in the same environmental conditions (*i.e.*, temperature, salinity, partial pressure of carbon dioxide [pCO_2], and food concentration). The first cohort was produced on July 5–6, 2018, and held in culture vessels specific to their date of fertilization. The second cohort was spawned on July 10, 2018, and divided between five culture vessels for use in scanning electron microscopy and observation of developmental transition. The use of multiple culture vessels across both cohorts ensured a continuation of the study in the event of complete culture vessel collapse.

To produce a cohort, gametes were obtained *via* strip spawning (Landau, 2014), where a small incision was made on the gonadal tissue located at the distal end of the bivalve foot. Gametes were observed under a light microscope to determine the sex of the brood-stock individual and the relative gonadal development stage. Eggs were collected from three females and added to 1-μm filtered seawater, then gently rinsed through a 153-μm mesh, a 63-μm mesh, and a 20-μm mesh, consecutively, to remove tissue and mucus from the eggs. The cleansed eggs were then removed from the mesh using a clean plastic transfer pipet

and suspended in 1-μm filtered seawater. The eggs were kept on ice for about 30 min, during which time sperm was excised from one male. While sperm counts were not conducted, sperm cells were assessed for viability, and fertilization was monitored to ensure that there was no evidence of polyspermy. The isolated sperm was diluted into 1 mL of 1-μm filtered seawater following excision. To initiate fertilization, 1 mL of sperm was then added to 400 mL of eggs at a concentration of 6180 eggs mL^{-1} and gently mixed. For both cohorts, each culture vessel was stocked at 10 larvae mL^{-1} using the gametes of three females and one male. The timing of each developmental phase was cataloged for each group as hours (HPF) or days (DPF) postfertilization to account for the influence of production date for each larval brood.

Larval culture

The first cohort was held inside two 3.79-L vessels with a 20-μm mesh bottom and placed in ambient seawater. Cohort 2 was divided among five 3.79-L vessels with 20-μm mesh bottoms, each placed inside two stacked vessels partially submerged in an aquarium tank to regulate temperature. The inner vessel had effluent holes covered in 63-μm mesh to allow for flow through, but the outer 7.57-L vessel prevented aquarium water from entering the culture vessel. Ambient seawater was introduced using a dripper placed at the bottom of the culture vessel, under the mesh holding the spawned embryos. Salinity and temperature were measured once daily. Once the feeding D-veliger stage was reached, live phytoplankton produced from cultures of haptophytes (Alutiiq Pride Marine Institute, Seward, AK) were administered three times a day at a level of 150 cells $larva^{-1}$, per culture vessel, as per hatchery feeding protocol. Larvae were gently suspended in the water column, and the bottom of the 20-μm mesh was cleaned once weekly with 6.3-mm Tygon tubing (Saint-Gobain Life Sciences, Courbevoie, France), using vacuum pressure to remove any accumulated detritus. Both cohorts were reared at 10.5 ± 1 °C and a salinity of 31.3 ± 0.2, with cohort 1 being viable to 21 days and cohort 2 viable to 28 days. The aragonite saturation state was 1.72 ± 0.23.

Biometric shell measurements

Larval cultures were subsampled every hour for the first 12 h until embryo hatching and then every 4 h for the following 68 h for analysis using light microscopy. At the 80-h mark, when the D-veliger stage was reached, microscopic observations were made every 24 h to ensure the availability of larvae for future sampling. After 9 DPF, observations were made every 3 days until day 21, when the D-veligers exhibited a very slight rounding at the umbo, signaling metamorphosis. Cohort 1 was not viable past 21 days, but a final light microscopy sample was collected on day 28 from cohort 2.

A photographic survey of developmental stages was generated over 28 days by imaging individuals from cohort 1 using light microscopy (an individual from cohort 2 was photographed for day 28). At each sampling time point, a subsample from each developmental culture vessel was siphoned from the vessel and held on ice during microscopy imaging. Larvae were placed in a 15-mL Falcon tube (Corning, Corning, NY) from which 40 μL were subsampled and deposited on a microscope slide. Microscope slides were equipped with petroleum jelly feet to allow individuals to maintain native conformation. After initial observation, individuals were fixed in 70% ethanol and imaged through a light microscope. Image analyses included measurements of length, width, and area using Fiji image analysis software (Schindelin *et al.*, 2012). The timing of each developmental transition was also noted.

Shell morphology

On days 7, 14, 21, and 28, individuals were harvested to examine shell growth and topography using scanning electron microscopy. A small subsample of larvae was extracted from each culture vessel of cohort 2, using larval condensation and siphoning, then examined under a light microscope to ensure viability (*via* larval activity and internal food presence) at the time of sampling. Following the initial examination, a portion of the subsample was deposited into a 2-mL cryovial and fixed with 500 μL of 70% ethanol to preserve the crystalline structure of the calcium carbonate present (Setoguchi *et al.*, 1989; Weiner *et al.*, 2003). These samples were examined at the Advanced Instrumentation Laboratory at the University of Alaska Fairbanks, using the FEI Quanta 200 scanning electron microscope (Hillsboro, OR; hereafter, SEM) outfitted with iXRF software and hardware and an e2v SSD energy-dispersive X-ray spectroscopy detector (Austin, TX).

A shell cleaning protocol using different fluid densities was developed to ensure the removal of all residual salt in preparation for iridium coating prior to SEM analysis. To begin, 500 μL of deionized water was added to each shell vial, which was then placed in a water bath and gently warmed to 28 °C for 5 min. Then 1500 μL of ice-cold deionized water was added and the vial inverted multiple times to mix the solution thoroughly. Each vial was centrifuged at 2000 × *g* to concentrate the larvae, and the top 1500 μL of supernatant was discarded. The periostracum was removed from the shell, using a hydrogen peroxide rinse (Green *et al.*, 2009). First, 500 μL of 3% hydrogen peroxide was added to each shell vial and incubated at 21 °C for 20 min, after which it was warmed to 25 °C in a water bath for 2 min and injected with 1000 μL of ice-cold deionized water. The vial was inverted multiple times and centrifuged, after which the top 1500 μL of supernatant was removed. Thermally induced density differences in rinse solutions facilitated the isolation and removal of the portion of the solution that contained the salt and ethanol. Prior to use on experimental shells, this preparation method was tested on a subsample of practice shells

Table 1

Timing of development of *Siliqua patula* at 10.5 ± 1 °C

Developmental stage	Timing postfertilization	Corresponding image (Fig. 1)
Polar body	80 MPF	A
First cleavage (two celled)	140 MPF	B
Second cleavage (four celled)	3 HPF	C
Third cleavage (eight celled)	5 HPF	D
Morula (16 celled)	6 HPF	E
Morula (32 celled)	7 HPF	F
Coeloblastula	11 HPF	G
Onset of embryo hatching	14 HPF	H
Newly hatched trochophore	30 HPF	I
Free-swimming trochophore	36 HPF	J–N
Onset of valve formation	73 HPF	O
Greater distinction during valve formation	76 HPF	P
D-veliger	80 HPF	Q
D-veliger	86 HPF	R
D-veliger	4 DPF	S
D-veliger, first indication of internal organ formation	8 DPF	T
D-veliger, distinct organ structures visible	12 DPF	U
D-veliger, velum protruding and active	15 DPF	V
D-veliger, hinge begins to round	18 DPF	W
D-veliger, early umbo formation visible	28 DPF	X

DPF, days postfertilization; HPF, hours postfertilization; MPF, minutes postfertilization.

to ensure that the cleaning process did not alter the shell morphology or composition. After cleaning, shells were mounted on SEM stubs, coated in 0.02 nm of iridium, and imaged under high-vacuum conditions using SEM.

Review of developmental timing of bivalves

To provide context for the developmental timing of *S. patula* relative to other bivalves, *S. patula* data, and data from Da Costa *et al.* (2008) and Da Costa *et al.* (2010)

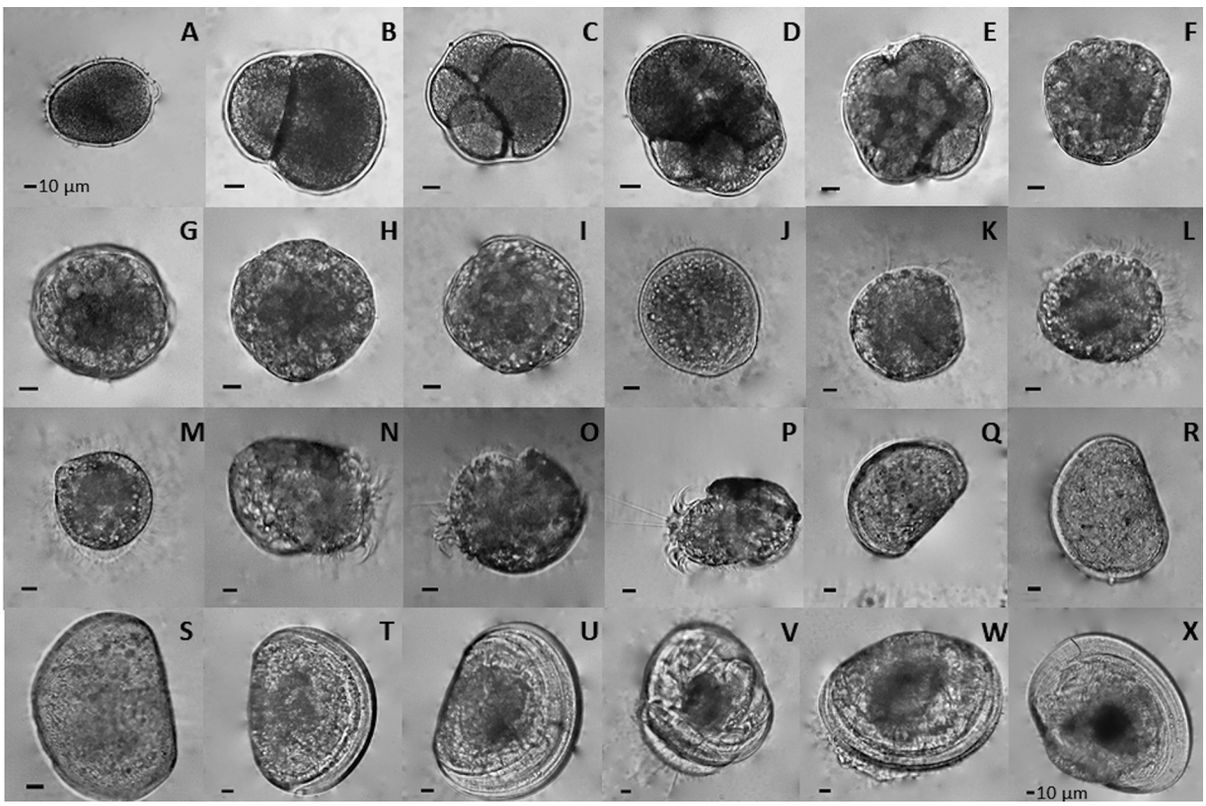

Figure 1. Developmental series of *Siliqua patula*. (A–G) Early embryos. (H–P) Trochophore stage. (Q–W) D-veliger stage. (X) Early pedi-veliger stage.

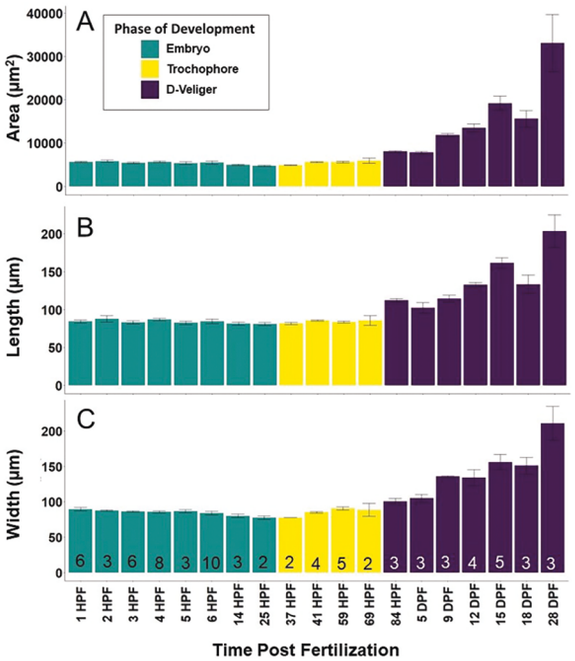

Figure 2. Size (±1 SD) of embryonic and larval *Siliqua patula* at 10.5 ± 1 °C over time. These data are representative of cohort 1. (A) Area (μm^2). (B) Length (μm). (C) Width (μm). Sample sizes (n) are at the level of individual and are listed for each time point at the bottom of each bar in (C). DPF, days postfertilization; HPF, hours postfertilization.

regarding *Ensis magnus* (previously *Ensis arcuatus*) and *Ensis siliqua*, respectively, were combined with the assembled bivalve data from Peck *et al.* (2007). Data reporting the size of trochophores upon initial hatching, as well as the timing and initial sizing of the D-veliger stage, were also included from the surveyed literature. This collated data will be referred to as the review dataset, hereafter.

Statistical analysis

Using Grubbs's tests, each category of the review dataset (timing to trochophore stage, average size of organism at trochophore emergence, timing of D-veliger stage, and average size at D-veliger emergence) was analyzed to identify potential outliers from the review dataset. Each Grubbs's test was conducted using R (R Development Core Team, 2013), through the Rstudio interface (ver. 1.4.1106). The α level was set to $P < 0.05$ for all analyses performed.

Results

Embryonic and larval development

Presented here is the first time line (Table 1) and photographic series of *Siliqua patula* development (Fig. 1). The eggs harvested had an average diameter of 61.6 ± 3.4 μm (n = 6). Similar to McMillin (1924), the eggs examined were either round or pear shaped and consisted of a white center surrounded by a gelatinous coating. The first polar body appeared 80 min after fertilization (Fig. 1A) and measured 15.6 μm^2 on average (n = 6). The first cleavage was observed at 140 minutes postfertilization (MPF) when the zygote divided into two unequally sized blastomeres (Fig. 1B). This is the first photographic validation that *S. patula* exhibits holoblastic spiral cleavage. At 3 HPF, embryos reached the four-cell stage, characterized by three blastomeres of identical size and a fourth, much larger blastomere, all surrounded by the vitelline coat (Fig. 1C). At 5 HPF, embryos achieved the eight-cell stage. At this phase, embryos were composed of seven micromeres and one macromere, all held within the vitelline coat (Fig. 1D). The 16-celled and 32-celled morula stages were reached at 6 and 7 HPF, respectively (Fig. 1E, F). The coeloblastula stage occurred at 11 HPF (Fig. 1G). At 14 HPF, the coeloblastula began moving rotationally, indicating the onset of embryonic hatching from the vitelline coat (Fig. 1H).

The first trochophores emerged at 30 HPF (Fig. 1I). Newly hatched trochophores did not appear to swim freely and instead oscillated in small circles. This was likely due to limited cilia or the uneven distribution of cilia present at this stage. At 36 HPF, the trochophore cilia were much more developed and abundant, as demonstrated by the presence of freely swimming individuals (Fig. 1J–N). The first evidence of valve formation was observed at 73 HPF (Fig. 1O), with valves becoming more distinct at 76 HPF (Fig. 1P).

Free-swimming, straight-hinged D-veligers appeared at 80 HPF (Fig. 1Q–S) and were observed successfully feeding. Moreover, growth during the D-veliger phase was pronounced (Fig. 2). Internal organ structures were first noted at 8 DPF, although distinct structures were slightly ambiguous (Fig. 1T). These initial organ structures were distinct in form at 12 DPF (Fig. 1U). Following the development of internal organs, D-veligers exhibited pronounced velum development by 15 DPF, demonstrated by the distinct protrusion of the velum during feeding behavior and swimming (Fig. 1V). The first indication of umbification in the *S. patula* larva occurred at 18 DPF (Fig. 1W), with recognizable umbification present at 28 DPF (Fig. 1X).

Mean larval area, length, and width were 5412 ± 353.8 μm^2, 84 ± 2.6 μm, and 85 ± 3.6 μm, respectively (n = 8; Fig. 2). Notable changes in all size metrics occurred at the D-veliger stage, with an average area of 15,589 ± 8713.8 μm^2, an average length of 137 ± 35.1 μm, and an average width of 142 ± 36.9 μm (n = 7) across the D-veliger stage.

Shell formation

The SEM analysis of *S. patula* on 7, 14, 21, and 28 DPF revealed the developmental progression and growth of the prodissoconch I (PDI; Fig. 3). Remarkably, SEM analysis also established that *S. patula* utilizes a concretion, or a flexible organic matrix that slowly incorporates a more mineralized form once tissue structures become specialized, during PDI development (Fretter and Pilkington, 1971). On day 7

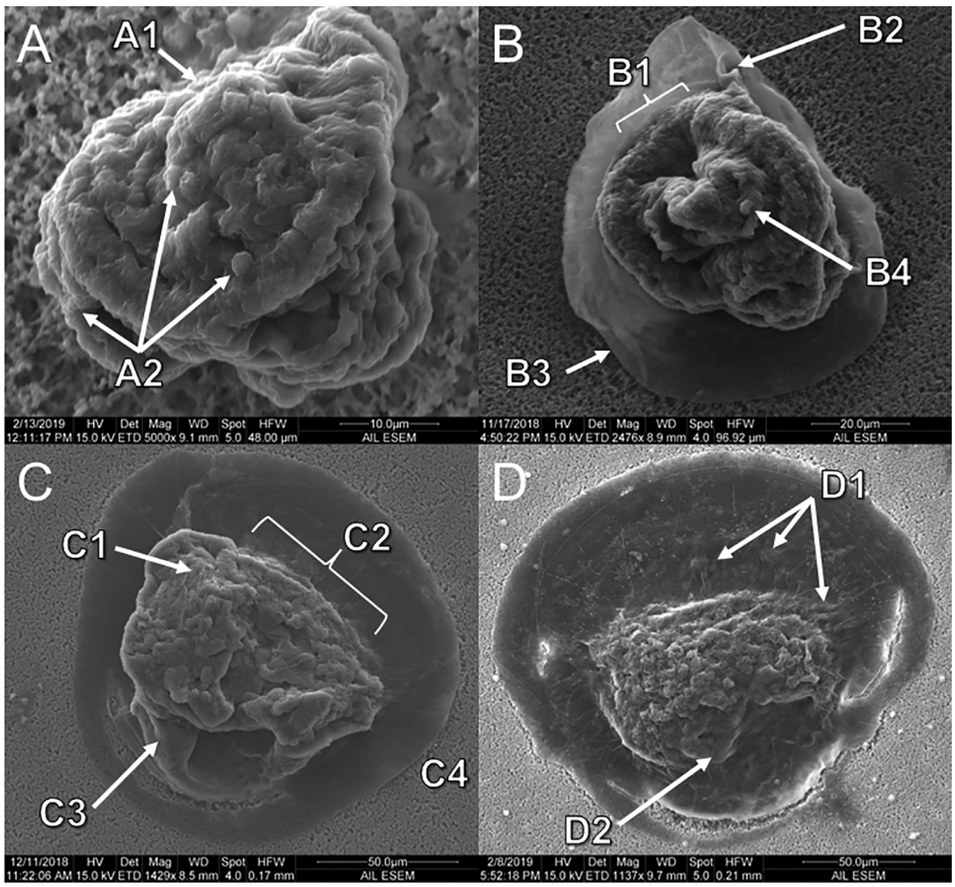

Figure 3. The concretion progression of *Siliqua patula*. Scanning electron microscope micrographs of shell size and morphology at 7 (A), 14 (B), 21 (C), and 28 (28) days postfertilization (DPF). (A1) Hinge side of the larva. (A2) Globular concretion nodes evident. (B1) First instance of the mineral front. (B2) Flexing of the extending concretion on the hinge side of the larva. (B3) Bending at the leading edge, highlighting concretion flexibility. (B4) Globular structure still present. (C1) Nodes appeared more crystallized, indicating an increase in mineral deposition. (C2) Progression of mineral front toward leading edge. (C3) Smoothing of surface topography also indicated advancement in mineralization. (C4) Loss of flexion along concretion edge. (D1) Further expansion of mineral front with concretion nodes present. (D2) Progression of smoothed surface topography.

(Fig. 3A), the mean PDI area was $1807 \pm 956\ \mu m^2$ ($n = 13$; Fig. 4). At this point, the PDI appeared as a rough and bumpy amalgamation of elemental constituents, accompanied by long globular calcification structures that covered the shell surface, characteristic of a concretion (Fig. 3A). By day 14 (Fig. 3B), the globular braided features of the concretion were still present; however, the development of a smoother shell surface was visible along the rim, with a mean shell area of $2843.5 \pm 1622\ \mu m^2$ ($n = 8$; Fig. 4). Though individuals at 14 DPF more closely resembled a typical larval bivalve shell, their shells still appeared to be structurally flexible. This was evident in the curling and bending present along the rim and hinge (Fig. 3, B2, B3). Additionally, by day 14, a mineral front had appeared as a transitional zone between the globular concretion structure and the smoother leading edge of the concretion (Fig. 3, B4). While shell appearance on day 21 (Fig. 3C) was similar to that on day 14 (Fig. 3B), the day 21 shell was much larger, with an average area of $11{,}566 \pm 5935\ \mu m^2$ ($n = 9$; Fig. 4). Furthermore, the shell edge no longer had the bending and curling appearance of the 14-day shell (Fig. 3, C4). There was also an increase in the crystalline appearance of the mineral concretion nodes (Fig. 3, C1) and a change in concretion topography, as the surface also appeared to have smoothed out slightly, with larger nodes covering the concretion surface (Fig. 3, C3). The mineral front had also increased in size by day 21 (Fig. 3, C2). By day 28 (Fig. 3D), mean shell area was $17{,}742 \pm 6906\ \mu m^2$ ($n = 8$; Fig. 4). While, visually, the day 28 concretion still resembled that on day 21, the mineral front was still present (Fig. 3, D1), although it had grown and extended toward the leading edge. The smoothed nodules were still evident toward the hinge (Fig. 3, D2), consistent with the larva on day 21.

Review of developmental timing of bivalves

A nonlinear model was fitted for both timing to the trochophore stage ($y = 172.24x^{-0.78}$, $R^2 = 0.7697$) *versus* temperature and timing to the D-veliger stage ($y = 648.45x^{-0.97}$, $R^2 = 0.6225$; Fig. 5) *versus* temperature. *Siliqua patula* development was comparable to other bivalve species (Peck *et al.*,

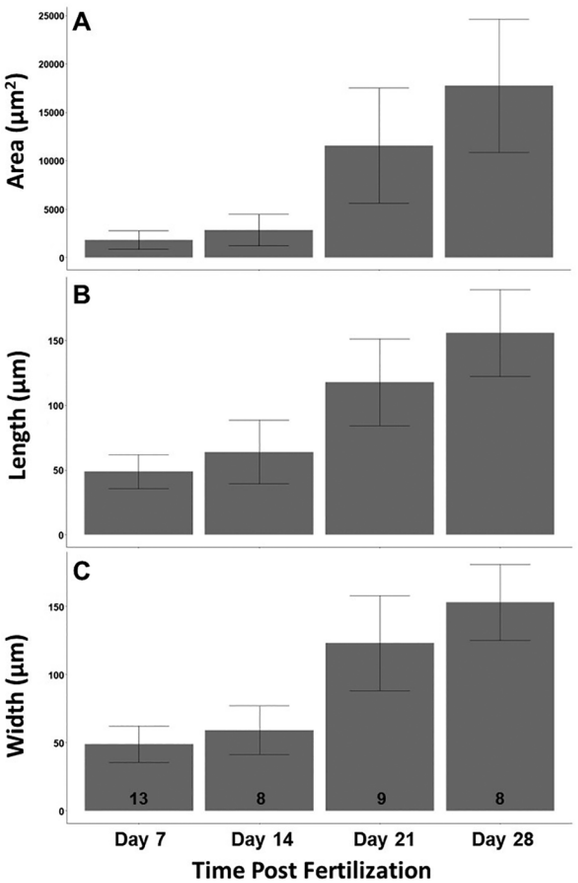

Figure 4. Shell size (±1 SD) of *Siliqua patula* from cohort 2, imaged using scanning electron microscopy on days 7, 14, 21, and 28. (A) Area (μm^2). (B) Length (μm). (C) Width (μm). Sample sizes (n) are at the level of individual and are listed for each time point at the bottom of each bar.

2007). Within the Pharidae family, both *Ensis magnus* and *S. patula* exhibited holoblastic spiral cleavage (embryology was not documented for *Ensis siliqua*). One major difference between the three Pharidae species is that neither *E. siliqua* nor *E. magnus* was successfully reared when spawned with a strip-spawning technique (Da Costa *et al.*, 2008, 2010). This finding has important implications for mariculture, as it appears that spawning techniques may be more species specific than previously assumed.

There were differences in developmental timing between *E. magnus* and *S. patula*. *Ensis magnus* reached the trochophore stage in 19 HPF, and *S. patula* took 30 HPF (the timing of *E. siliqua* was not reported). For *E. magnus* and *E. siliqua*, the D-veliger phase was reached at 30 and 24 HPF, respectively, compared to the 80 HPF that *S. patula* took to reach the D-veliger stage of development. *Siliqua patula* was reared at 10.5 ± 1 °C, compared to 18 °C for *E. magnus* and 19 °C for *E. siliqua*. While the size of individuals within the Pharidae family appeared to be consistent with the species listed by Peck *et al.* (2007), *S. patula* was 20 μm longer, on average, than *E. magnus* at the onset of the trochophore stage.

Discussion

This study provides valuable information regarding *Siliqua patula* and Pharidae development and relates Pharidae members to other bivalves in terms of developmental timing and size, as well as establishes an informational foundation for *S. patula* management, culturing practices, and research in the future. *Siliqua patula* follows typical bivalve development with the onset of the trochophore and D-veliger stages occurring at 30 and 80 HPF, respectively. *Siliqua patula* does differ, however, in the formation of a concretion. Additionally, the majority of *S. patula* growth occurs during the D-veliger stage, concurrent with the onset of feeding behavior. Moreover, both the timing of development and *S. patula* size are consistent with those reported in a global assemblage of bivalves compiled by Peck *et al.* (2007).

Larval *S. patula* did not undergo the well-characterized shell formation process documented in other bivalve species such as *Laternula eliptica*, *Codakia orbicularis*, *Pinctada margaritifera*, or *Panopea zelandica* (Gros *et al.*, 1997; Doroudi and Southgate, 2003; Gribben and Hay, 2003; Bylenga *et al.*, 2017), which is first marked at the D-veliger stage by the formation of a smooth, calcified PDI, followed by an abrupt transition to the prodissoconch II (Kraeuter and Castagna, 2001). *Siliqua patula* differs from other bivalves, including *Ensis magnus*, another member of the Pharidae family, by exhibiting a braided, highly irregular PDI surface (Fig. 3A; Da Costa *et al.*, 2008). In fact, in direct contrast to the smooth, calcified shell evident on SEM micrographs of newly formed D-veligers of other bivalve species, including *E. magnus*, *S. patula* D-veligers possess a thicker and morphologically irregular PDI (Fig. 3). Furthermore, the developing *S. patula* larvae still lack the symmetry and smooth appearance present in other larval bivalve shells on day 28 of development. This mode of shell development, termed a concretion (Fretter and Pilkington, 1971), is characterized by an initial shell formed primarily by an organic matrix that provides the framework for the subsequent deposition of calcium carbonate. The use of a concretion delays complete calcification until later in development, with this time delay being highly species specific and possibly a result of either a stepwise process or a response to environmental conditions (Eyster, 1986). A concretion is potentially more flexible than a shell that is mineralized upon initial formation but still contains calcium as an elemental constituent (Eyster and Morse, 1984). Molluscs that produce a concretion typically develop a mineralized shell by the time of metamorphosis as the concretion crystallizes over time (Fretter and Pilkington, 1971).

Several freshwater bivalves are known to produce a concretion, which may be more common in environments with lower calcium concentrations or reduced ion availability (Hinzmann *et al.*, 2015). Concretions are also more commonly found among gastropods to allow a certain degree of flexibility during their initial torsion while still

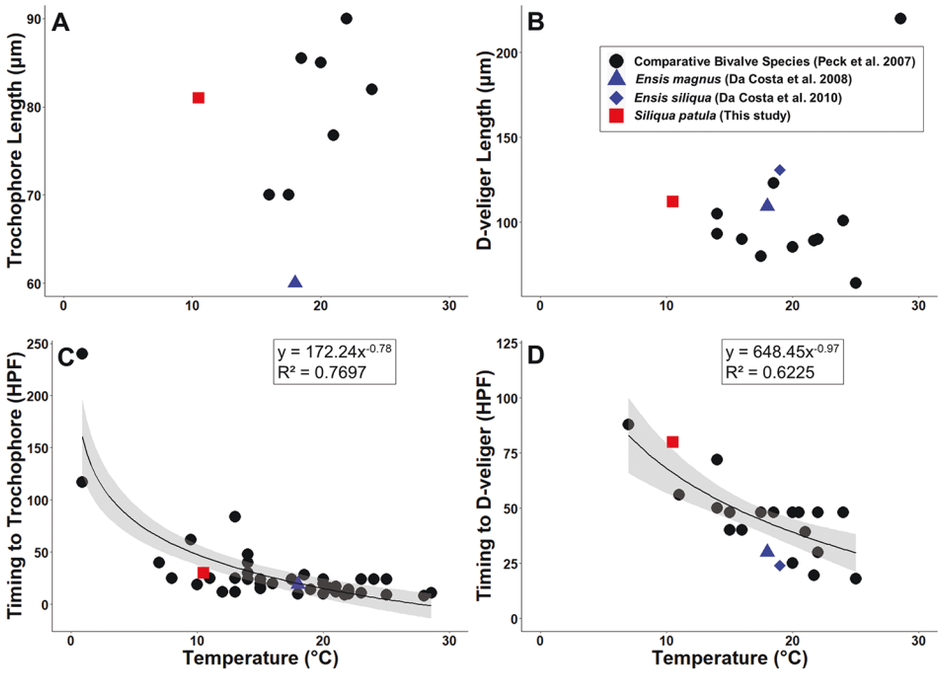

Figure 5. Comparison of *Siliqua patula* to globally dispersed bivalve species across a range of ambient temperatures. The gray area represents a 95% confidence interval (C, D). (A) Average size of individuals at trochophore emergence. (B) Average size of individuals at D-veliger emergence. (C) Time (hours postfertilization [HPF]) elapsed until trochophore emergence. (D) The time (HPF) elapsed until D-veliger emergence.

maintaining structure and support (Fretter and Pilkington, 1971). The utilization of shell characteristics more commonly found in gastropods and freshwater bivalves suggests that *S. patula* may be using a concretion technique to allow for shell flexibility during early shell development or as a compensatory mechanism to deal with reduced ion availability in their environment. Further experimentation is needed to definitively understand the evolutionary forces that result in *S. patula* using a concretion *versus* a more common calcium carbonate shell seen in other bivalves during their early D-veliger phase. However, given that bivalves do not undergo torsion, or immense shell morphological change during development, it appears unlikely that shell flexibility is the probable cause for concretion production. For *S. patula*, it may be a response to environmental conditions. The geographic distribution of *S. patula* spans the western coast of North America, from Alaska to California, inhabiting a wide range of coastal habitats (Alaska Department of Fish and Game, 2020). The population of clams sampled for this study occurs in an estuarine environment with a large amount of freshwater input by many sources, including glacial and riverine input as well as some of the highest freshwater submarine groundwater discharge on the planet (Haag *et al.*, 2023). This means that *S. patula* in this region is potentially experiencing reduced ion availability compared to individuals that live outside of an estuarine environment. This question is further fueled by research regarding the freshwater gastropod *Helisoma duryi*, which has been shown to both delay calcification *via* a concretion until posthatch and undergo calcification prior to hatching, depending on the study in question (Kapur and Gibson, 1967, 1968; Eyster, 1986). Further studies are needed to determine whether the formation of a concretion is a phenotypically plastic trait related to the environment or whether it is universally employed by *S. patula*.

When compared to global data, *S. patula* follows the common embryonic and larval developmental trajectory seen in other bivalve species and aligns with the size of other members of the Pharidae family previously studied, *E. magnus* and *Ensis siliqua*. The longer developmental times of *S. patula* compared to the other two members of the Pharidae are likely explained by the colder temperature at which the *S. patula* larvae were cultured, as temperature is the main driver of the speed of development in marine invertebrates (Hoegh-Guldberg and Pearse, 1995). While this finding bolsters the established knowledge regarding Pharidae developmental timing and larval growth, it is crucial to note that to date, only four studies (including this one) have documented information for this family (Breese and Robinson, 1981; Da Costa *et al.*, 2008, 2010).

Conclusions

While *S. patula* appears to follow a well-characterized bivalve developmental trajectory, including developmental timing and growth, this species deviates largely from other bivalves in its initial shell formation. This discovery underscores the importance of high-magnification and high-resolution shell analysis for several reasons. First, this

characteristic may not have been detected due to the inability of light microscopy to resolve shell surface topology. Second, any indications of flexibility or crystalline presence were only distinguishable using SEM micrographs. Last, assumptions about concretion use cannot be made from shell transparency under light observation (Eyster and Morse, 1984). This study is direct evidence of the necessity of SEM analysis during studies of larval bivalve development.

This study also exposes the need for further research into larval shell development on members of the Pharidae family to determine whether the use of a concretion is evolutionarily conserved within the family or solely an adaptation of *S. patula*. Certain members of the Pharidae family have adapted to inhabit freshwater (Bolotov *et al.*, 2018). It should, therefore, be determined whether the concretion is an example of phenotypic plasticity within the species as a result of environmental pressure or a family-wide developmental trait that favors habitation in estuarine or freshwater environments. Given the global distribution of and economic, cultural, and alimentary value of Pharidae bivalves, they warrant a more vested interest in the details of their development. Complete characterization of additional Pharidae members, including SEM analysis of *E. magnus* and *E. siliqua* would inform management decisions and aid mariculture efforts, increasing rearing success and potentially helping bolster previously reduced populations.

Further research is critical to achieve a better understanding of *S. patula* and Pharidae family development, especially since bivalves such as *S. patula* are expected to be vulnerable to ocean change in the future, particularly ocean acidification (Fabry *et al.*, 2008). This vulnerability is especially pronounced during early life stages (Waldbusser *et al.*, 2015). To date, only one study (Alcantar *et al.*, 2024) appears to have examined how concretion-utilizing bivalves will respond to changes in the carbonate system. This large knowledge gap reinforces the need for comprehensive studies of bivalve development in concert with thorough examinations of the impacts of ocean change stressors to accurately inform the discussion of bivalve health within the context of a changing ocean.

Acknowledgments

We would like to acknowledge that this study was conducted by researchers working and residing on the unceded traditional homelands of the Lower Tanana Dené and that the study itself was conducted on the unceded traditional homelands of the Sugpiaq/Alutiiq People in their community of Qutalleq. We are grateful to the staff of the Alutiiq Pride Marine Institute and the Chugach Regional Resources Commission. We thank Dr. Cale Miller, Shelby Bacus, Josianne Haag, Jonah Jossart, and James Currie of the Kelley lab as well as Dr. Ken Severin and Nathan Graham of the Advanced Instrument Laboratory at the University of Alaska Fairbanks. The Alutiiq Pride Marine Institute, the Rasmuson Fisheries Research Center, Alaska EPSCoR Program, National Science Foundation award OIA-1757348, the Cooperative Institute for Alaska Research, and the Robert and Kathleen Byrd Award financially supported M.W.A. and this research.

Literature Cited

Alaska Department of Fish and Game. 2020. Razor clam (*Siliqua patula*). Available: https://www.adfg.alaska.gov/index.cfm?adfg=razorclam.main [2024, May 15].

Alcantar, M. W., J. Hetrick, J. Ramsay, and A. L. Kelley. 2024. Examining the impacts of elevated, variable pCO_2 on larval Pacific razor clams (*Siliqua patula*) in Alaska. *Front. Mar. Sci.* **11:** 1253702.

Ayres, D. 2022. Washington Razor Clam Management. [Online]. Washington Department of Fish and Wildlife. Available: https://wdfw.wa.gov/publications/02334 [2024, May 15].

Bolotov, I. N., I. V. Vikhrev, M. Lopes-Lima, Z. Lunn, N. Chan, T. Win, O. V. Aksenova, M. Y. Gofarov, A. V. Kondakov, E. S. Konopleva *et al.* 2018. Discovery of *Novaculina myanmarensis* sp. nov. (Bivalvia: Pharidae: Pharellinae) closes the freshwater razor clams range disjunction in Southeast Asia. *Sci. Rep.* **8:** 16325.

Breese, W. P., and A. Robinson. 1981. Razor clams, *Siliqua patula* (Dixon): gonadal development, induced spawning and larval rearing. *Aquaculture* **22:** 27–33.

Bylenga, C. H., V. J. Cummings, and K. G. Ryan. 2017. High resolution microscopy reveals significant impacts of ocean acidification and warming on larval shell development in *Laternula elliptica*. *PLoS One* **12:** e0175706.

Da Costa, F., S. Darriba, and D. Martinez-Patino. 2008. Embryonic and larval development of *Ensis arcuatus* (Jeffreys, 1865) (Bivalvia: Pharidae). *J. Molluscan Stud.* **74:** 103–109.

Da Costa, F., D. Martínez-Patiño, J. Ojea, and S. Nóvoa. 2010. Larval rearing and spat production of the razor clam *Ensis siliqua* (Bivalvia: Pharidae). *J. Shellfish Res.* **29:** 347–351.

Dorit, R., W. F. Walker, and R. D. Barnes. 1991. *Zoology*, 1st edition. Brooks Cole, Philadelphia.

Doroudi, M. S., and P. C. Southgate. 2003. Embryonic and larval development of *Pinctada margaritifera* (Linnaeus, 1758). *Molluscan Res.* **23:** 101.

Eyster, L. S. 1986. Shell inorganic composition and onset of shell mineralization during bivalve and gastropod embryogenesis. *Biol. Bull.* **170:** 211–231.

Eyster, L. S., and M. P. Morse. 1984. Early shell formation during molluscan embryogenesis, with new studies on the surf clam, *Spisula solidissima*. *Integr. Comp. Biol.* **24:** 871–882.

Fabry, V. J., B. A. Seibel, R. A. Feely, and J. C. Orr. 2008. Impacts of ocean acidification on marine fauna and ecosystem processes. *ICES J. Mar. Sci.* **65:** 414–432.

Forster, Z. 2019. *Summary Report of the 2019 Commercial Fishery for Razor Clams* (Siliqua patula). Washington Department of Fish and Wildlife, Ocean Park.

Fretter, V., and M. C. Pilkington. 1971. The larval shell of some prosobranch gastropods. *J. Mar. Biol. Assoc. U.K.* **51:** 49–62.

Garcia de Severeyn, Y. G., H. Severeyn, W. Grant, and Y. Reverol. 2000. Effect of water temperature on larval development of the bivalve mollusk *Tivela mactroides*: evaluation in the laboratory and via simulation. *Ecol. Model.* **129:** 143–151.

Gilbert, S. F. 2000. *Developmental Biology*, 6th edition. Sinauer, Sunderland, MA.

Green, M. A., G. G. Waldbusser, S. L. Reilly, K. Emerson, and S. O'Donnell. 2009. Death by dissolution: sediment saturation state as a mortality factor for juvenile bivalves. *Limnol. Oceanogr.* **54:** 1037–1047.

Gribben, P. E., and B. E. Hay. 2003. Larval development of the New Zealand geoduck *Panopea zelandica* (Bivalvia: Hiatellidae). *N.Z. J. Mar. Freshw. Res.* **37:** 231–239.

Gros, O., L. Frenkiel, and M. Moueza. 1997. Embryonic, larval, and post-larval development in the symbiotic clam *Codakia orbicularis* (Bivalvia: Lucinidae). *Invertebr. Biol.* **116:** 86.

Haag, J., H. Dulai, and W. Burt. 2023. The role of submarine groundwater discharge to the input of macronutrients within a macrotidal subpolar estuary. *Estuar. Coasts* **46:** 1740–1755.

Hedgecock, D. 1995. The cupped oyster and the Pacific oyster. Pp. 115–137 in *Conservation of Fish and Shellfish Resources: Managing Diversity*, J. E. Thorpe, G. A. E. Gall, J. E. Lannan, and C. E. Nash, eds. Academic Press, London.

Hinzmann, M. F., M. Lopes-Lima, I. Bobos, J. Ferreira, B. Domingues, and J. Machado. 2015. Morphological and chemical characterization of mineral concretions in the freshwater bivalve *Anodonta cygnea* (Unionidae). *J. Morphol.* **276:** 65–76.

Hoegh-Guldberg, O., and J. S. Pearse. 1995. Temperature, food availability, and the development of marine invertebrate larvae. *Am. Zool.* **35:** 415–425.

Holderied, K., and S. Baird. 2020. Oceanographic conditions in lower Cook Inlet and Kachemak Bay. [Online]. Gulf Watch Alaska. Available: https://gulfwatchalaska.org/monitoring/environmental-drivers/oceanographic-conditions-in-lower-cook-inlet-and-kachemak-bay [2024, May 15].

Huang, B., P. W. Thorne, V. F. Banzon, T. Boyer, G. Chepurin, J. H. Lawrimore, M. J. Menne, T. M. Smith, R. S. Vose, and H.-M. Zhang. 2021. NOAA Extended Reconstructed Sea Surface Temperature (ERSST). [Online]. NOAA National Centers for Environmental Information. Available: https://www.ncei.noaa.gov/access/metadata/landing-page/bin/iso?id=gov.noaa.ncdc:C00927 [2024, May 15].

Hunter, M. 2024. Commercial Shellfishing. Available: https://www.dfw.state.or.us/mrp/shellfish/commercial/harvest_permit.asp [2024, May 15].

Kapur, S. P., and M. A. Gibson. 1968. A histochemical study of calcium storage in the foot of the freshwater gastropod, *Helisoma duryi eudiscus* (Pilsbry). *Can. J. Zool.* **46:** 987–990.

Kapur, S. P., and M. A. Gibson. 1967. A histological study of the development of the mantle-edge and shell in the freshwater gastropod, *Helisoma duryi eudiscus* (Pilsbry). *Can. J. Zool.* **45:** 1169–1181.

Kraeuter, J. N., and M. Castagna. 2001. *Biology of the Hard Clam*. Elsevier, Amsterdam.

Landau, B. J. 2014. The bin-silo system: a simple spawning method for bivalve shellfish. *World Aquacult.* **45:** 58–61.

McEdward, L. R. 1985. Effects of temperature on the body form, growth, electron transport system activity, and development rate of an echinopluteus. *J. Exp. Mar. Biol. Ecol.* **93:** 169–181.

McMillin, H. C. 1924. *The Life-History and Growth of the Razor Clam*. FM Lamborn, Public Printer, Olympia, WA.

Miller, C. A., and A. L. Kelley. 2021. Seasonality and biological forcing modify the diel frequency of nearshore pH extremes in a subarctic Alaskan estuary. *Limnol. Oceanogr.* **66:** 1475–1491.

NOAA (National Oceanic and Atmospheric Administration). 2023. Coastal Water Temperature, Northern Pacific Coast. [Online]. NOAA National Centers for Environmental Information. Available: https://www.ncei.noaa.gov/access/coastal-water-temperature-guide/all_table.html#npac [2024, May 15].

Olsen, L. 2015. Cause of razor clam decline remains mystery. [Online]. *Homer News*, Homer, AK. https://www.homernews.com/news/cause-of-razor-clam-decline-remains-mystery [2024, May 15].

Peck, L. S., D. K. Powell, and P. A. Tyler. 2007. Very slow development in two Antarctic bivalve molluscs, the infaunal clam *Laternula elliptica* and the scallop *Adamussium colbecki*. *Mar. Biol.* **150:** 1191–1197.

Phoa Lee Na, C. 2008. Morphological assessment and preliminary molecular work on "Ambal Goyang," *Psammobia rostratus* (Bivalvia). PhD dissertation, Universiti Malaysia Sarawak.

Ponder, W. F., D. R. Lindberg, and J. M. Ponder. 2019. *Biology and Evolution of the Mollusca*. CRC, Boca Raton, FL.

R Development Core Team. 2013. R: a language and environment for statistical computing. [Online]. R Foundation for Statistical Computing, Vienna. Available: http://www.R-project.org [2024, May 15].

Schindelin, J., I. Arganda-Carreras, E. Frise, V. Kaynig, M. Longair, T. Pietzsch, S. Preibisch, C. Rueden, S. Saalfeld, B. Schmid *et al.* 2012. Fiji: an open-source platform for biological-image analysis. *Nat. Methods* **9:** 676–682.

Setoguchi, H., M. Okazaki, and S. Suga. 1989. Calcification in higher plants with special reference to cystoliths. Pp. 409–418 in *Origin, Evolution, and Modern Aspects of Biomineralization in Plants and Animals*, R. E. Crick, ed. Springer, Boston.

Swanson, C. 2024. Razor clams, geoducks battle to be WA's top clam. [Online]. *Seattle Times*. Available: https://www.seattletimes.com/seattle-news/climate-lab/razor-clams-geoducks-battle-to-be-was-top-clam/ [2024, May 15].

Waldbusser, G. G., B. Hales, C. J. Langdon, B. A. Haley, P. Schrader, E. L. Brunner, M. W. Gray, C. A. Miller, and I. Gimenez. 2015. Saturation-state sensitivity of marine bivalve larvae to ocean acidification. *Nat. Clim. Change* **5:** 273–280.

Weiner, S., Y. Levi-Kalisman, S. Raz, and L. Addadi. 2003. Biologically formed amorphous calcium carbonate. *Connect. Tissue Res.* **44:** 214–218.